VELOCITY AND WALL SHEAR STRESS MEASUREMENTS IN VERY SMALL CHANNELS BY AN ULTRASOUND PULSED VELOCIMETER BASED TECHNIQUE

Anna Paraboschi, Enrico Orsi
D.I.I.A.R. Politecnico di Milano, piazza Leonardo da Vinci 32, 20133 Milan, Italy
anna.paraboschi@polimi.it, enrico.orsi@polimi.it

Abstract:

In this study we present the analysis of a turbulent boundary layer for the Reynolds number (Re) range: $6{,}8 \cdot 10^3 < Re < 10{,}8 \cdot 10^3$, in a smooth rectangular channel, by the use of a Pulsed Ultrasound Doppler Velocimeter.
This technique enables us to acquire velocity profiles along the direction of the sound in short intervals of time (order of magnitude: ms) obtaining, in this way, a very high spatial and temporal resolution, and, as a consequence, allowing us to do measurements of velocity profiles in a very short time.
This study has been developed for a pressure driven flow.
The goals pursued doing the experiments have been:

- to determine the local value of the wall shear stress on the centre of the channel (τ_{CL}) analyzing the velocity profile;
- to evaluate the reliability of this methodology: the results have been compared with those derived by the measurements carried out by a Preston tube. The mean difference between the two measurements has been of 14 % with also tolerances of 3%-6%;
- to determine the wall shear stress on the centre of the sidewall (τ_{sw}) by the use of a Preston tube and then:
  - to analyze the dependence of the ratio between the wall shear stress estimated at the centre line of the bottom and the one measured on the sidewall centre line on the Reynolds number of the flow;
  - to evaluate the relationship between the local wall shear stresses and the mean wall shear stress (τ_{mean}) with the "aspect ratio" of the cross section comparing the results with the ones published in literature.

Key words: Ultrasonic Doppler method, Pulsed ultrasound, Turbulent boundary layer flow, Log law, Wall shear stress, Area velocity.

1. Introduction:

The study of a flow field has a great importance in fluid dynamics about the analysis of the wall shear stress distribution, and the mechanisms of dissipation of energy both from the aerodynamic and hydraulic point of view.
The knowledge of the distribution of boundary shear stress is very important if we consider the role that both the local and the mean boundary shear stress have got in many engineering problems concerning, for instance, the wall resistance, the sediment transport, etc. (*Guo and Julien, 2005, Knight et al., 1984,1985*).
The distribution of boundary shear stress around the wetted perimeter of an open channel is known to be a function of the geometry of the cross section, the characteristics of the secondary flow cells, and any non uniformity in the boundary roughness (*Knight et al., 1984, Jin et al., 2004*).

Notwithstanding all the lavished efforts it is not easy yet to model the distribution of the wall shear stresses, and we can find recent researches in this field (*Yang and McCorquodale, 2004; Yang, 2005*).
From these observation comes the need to have a fair set of experimental results to give validity to the mathematical models.
The mean fully developed flow field in a pipe or in a channel has got only one component in the direction of the mean flow (u) that depends upon the distance from the wall.
In particular using the "inner variables" defined as:

- $y^+ = \frac{yu^*}{\nu}$ characteristic length scale, being:
  - y, the distance from the wall;
  - u*, the friction velocity equal by definition to $\sqrt{\frac{\tau_w}{\rho}}$, square root of the ratio between the wall shear stress and the density of the fluid;
  - ν, the cinematic viscosity of the fluid;
- $u^+ = \frac{u}{u^*}$ characteristic velocity scale;

It is traditionally admitted that for a turbulent boundary layer:

$$\frac{u}{u^*} = \frac{yu^*}{\nu} \tag{1}$$

for values of y^+ less than 5, therefore in the region known as the "viscous sublayer";
while for y^+ above 50:

$$\frac{u}{u^*} = \frac{1}{k}\ln\left(\frac{yu^*}{\nu}\right) + C \tag{2}$$

where k is the Von Kàrmàn's constant, usually considered equal to 0,41, while C is set equal to 5,2 (*Zagarola and Smits, 1998*). Nevertheless we have to say that at the varying of the experiments these variables, considered universal, change their value as shown in Tab.1.

Authors	**year**	**1/k**	**C**
Klebanoff	*1954*	2,44	4,9
Townsend	*1956*	2,44	7
Steffler et al.	*1985*	2,5	5,5
Nezu & Rodi	*1986*	2,43	5,29
Kirkgöz	*1989*	2,44	5,5
McKeon et al	*2004*	2,38	5,6
Zanoun et al.	*2003*	2,72	3,68
Österlund et al.	*2000*	2,60	4,17

Tab. 1: different values for the parameters 1/k e C.

Fig. 1 reproduces the trend of equations (1) and (2) from which emerges that between y^+ equal to 5, and y^+ equal to 50, there is a transition zone known as "buffer layer".

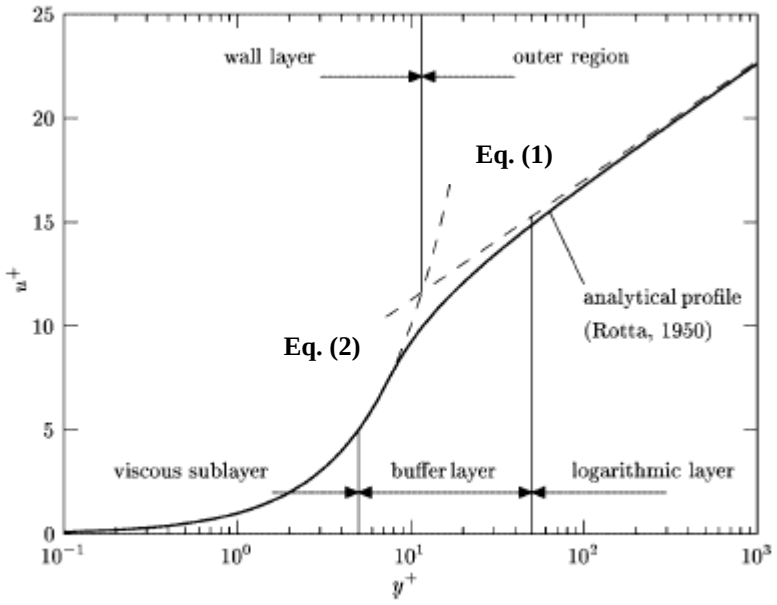

Fig. 1: normalized velocity profile in the boundary layer of a turbulent water flow (Nowak, 2002).

The use of equations (1) and (2) allows the evaluation of the wall shear stress because if we have a velocity profile that can be considered representative for the viscous sublayer, knowing a local velocity value at a distance far form the wall y, it is possible to calculate the friction velocity , and, as a consequence, the local value of the wall shear stress; otherwise, if we have more data points, it is possible to determine the unknown vale by a regression analysis bounded to the origin.
Analogously if we use equation (2) we can admit known the values of k and C and to calculate, knowing the velocity profile near the wall ($\frac{50 \cdot \nu}{u*}$<y < 0,15 R, where R is a characteristic length as , for example, the pipe's radius) and using the same method above mentioned, the wall shear stress, otherwise we can make a regression with two parameters to evaluate, for example, both the friction velocity value and the constant C.
In the following we are going to use the first methodology, and we will compare the values estimated with those coming both from Preston tube measurements, and literature data.

2. Ultrasound Doppler technique

Doppler ultrasound technique, was originally applied more than 30 years ago in the medical field. The use of pulsed emissions has extended this technique to other fields opening the way to new measuring techniques in fluid dynamics. The term "Doppler ultrasound velocimetry" implies that the velocity is measured by finding the Doppler frequency in the received signal, as it is the case in Laser Doppler velocimetry. In fact, in ultrasonic pulsed Doppler velocimetry, this is never the case because velocities are derived from shifts in positions between pulses, and the Doppler effect plays a minor role.

2.1 Principle of functioning of a "Pulsed Doppler ultrasound"

In pulsed Doppler ultrasound, instead of emitting continuous ultrasonic waves, an emitter sends periodically a short ultrasonic burst and a receiver collects continuously echoes issues from targets, or particles, that may be present in the path of the ultrasonic beam. By sampling the incoming echoes at the same time relative to the emission of the bursts, the shift of positions of scatters are measured. Let assume a situation, as illustrated in Fig.2, where only one particle is present along the ultrasonic beam.

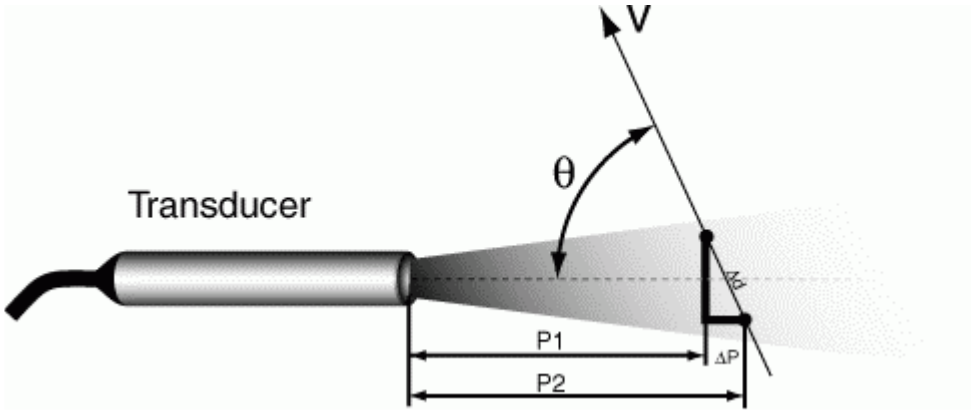

Fig.2 : scheme of the principle of functioning of a " Pulsed Ultrasound Doppler velocimeter" (Signal Processing S.A. DOP 2000 Model 2125 User's manual).

From the knowledge of the time delay T_d between an emitted burst and the echo issue from the particle, the depth, p, of this particle can computed by:

$$p = \frac{c \cdot T_d}{2}$$

where c is the sound velocity of the ultrasonic wave in the liquid. If the particle is moving at an angle θ regarding the axis of the ultrasonic beam, its velocity can be measured by computing the variation of its depth between two emissions separated in time by T_{prf}:

$$\left(P_2 - P_1\right) = v \cdot T_{PRF} \cdot \cos\theta = \frac{c}{2} \cdot \left(T_2 - T_1\right)$$

The time difference (T_2-T_1) is always very short, most of the time lower than a microsecond, and as a consequence it is advantageous to replace this time measurement by a measurement of the phase shift of the received echo:

$$\delta = 2\pi \cdot f_e \cdot \left(T_2 - T_1\right)$$

Being f_e the "emitting frequency".

We can therefore write that the velocity of the particle or "target":

$$v = \frac{c \cdot \delta}{4\pi \cdot f_e \cdot \cos\theta \cdot T_{PRF}} = \frac{c \cdot f_d}{2 \cdot f_e \cdot \cos\theta}$$

This last equation gives the same result as the Doppler equation. But one should always be aware that the phenomena involved are not the same. Assume that the particles are randomly distributed inside the ultrasonic beam. The echoes issue from each particle are then combined together in a random fashion, giving a random echo signal. Hopefully, a high degree of correlation exists between different emissions. This high correlation degree is put in advance in all digital processing techniques used in Signal Processing's Ultrasonic Doppler velocimeter to extract information, such as the velocity (*Signal Processing S.A. DOP 2000 Model 2125 User's manual).*

2.2 Advantages and limitations

The main advantage of pulsed Doppler ultrasound is its capability to offer spatial information associated to velocity values. Unfortunately, as the information is available only periodically, this technique suffers from the Nyquist's theorem. This means that a maximum velocity exists for each "pulse repetition frequency" (PRF):

$$V_{\max} = \frac{c}{4 \cdot T_{PRF} \cdot f_e \cdot \cos\theta}$$

In addition to the velocity limitation, there is a limitation in depth. The ultrasonic burst travels in the liquid at a velocity which depends on the physical properties of the liquid. The pulse repetition frequency gives the maximum time allowed to the burst to travel to the particle and back to the transducer. This gives a maximum depth of:

$$P_{\max} = \frac{T_{PRF} \cdot c}{2}$$

From the above two equations, we can see that increasing the time between pulses (T_{PRF}) will increase the maximum measurable depth, but will also reduce the maximum velocity which can be measured. The maximum velocity and maximum depth are thus related according to the following equation (*Signal Processing S.A. DOP 2000 Model 2125 User's manual).*:

$$P_{\max} \cdot V_{\max} = \frac{c^2}{8 \cdot f_e \cdot \cos\theta}$$

2.3 Ultrasound scattering

Ultrasound Doppler velocimetry requires a certain amount of particles suspended in the liquid, which may disturb its flow or change its fundamental properties.
Ultrasound attenuates as it progresses through a medium, i.e. its amplitude and intensity decrease gradually with increasing distance of travel. Assuming no major reflections, the main causes of attenuation are the following: scattering, diffraction and absorption. Attenuation is important because it limits the depth range especially with high-frequency sound beams. The rate of attenuation, or attenuation coefficient, depends on both the matter traversed and the ultrasound frequency. The rate of attenuation increases with increasing frequency. Attenuation can be compensated in the receiving amplifier by electronic circuitry which applies increasing gain as signals are received from increasing depths. The frequency dependence of attenuation results in the high frequency components of an ultrasonic pulse being preferentially reduced in amplitude relative to the low frequency components. The ultrasonic waves generated by the standard single-element transducer are more or less confined in a narrow cone. As they travel in this cone they may be scattered when they touch a particle having different acoustic impedance.

The acoustic impedance is defined by:

$$z = \rho \cdot c$$

where ρ is the density and c the sound velocity.
When an ultrasonic wave traveling through a medium strikes an acoustic interface, i.e., a discontinuity or any variation from uniformity in the medium of dimensions similar to or less than a wavelength, some of the energy of the wave is scattered in many directions.
Scattering is the process of central importance, since it provides most of the signals for echo Doppler techniques as in the case of pulsed Doppler ultrasound velocimetry.
If the size of the particle is bigger than the wave length, the ultrasonic waves are reflected and refracted by the particle. In such a case the direction of propagation and the intensity of the ultrasonic waves are affected. But if the size of the particle is much smaller than the wave length an other phenomena appears, which is named scattering. In such a case, a very small amount of the ultrasonic energy is reflected in all directions. The intensity and the direction of propagation of the incoming waves are practically not affected by the scattering phenomena. Ultrasonic Doppler velocimetry needs therefore particles smaller than the wave length (*Signal Processing S.A. DOP 2000 Model 2125 User's manual).*

3. Wall data correction

Nevertheless for a right reconstruction of the velocity profiles we have to take into considerations two aspects:

1) the sound beam has to cross different medium with differentiated sound characteristics, and, as a consequence, we have to place correctly the echoes to take into consideration the crossing of the two interfaces: gel-wall and wall-flow. (Fig. 3)

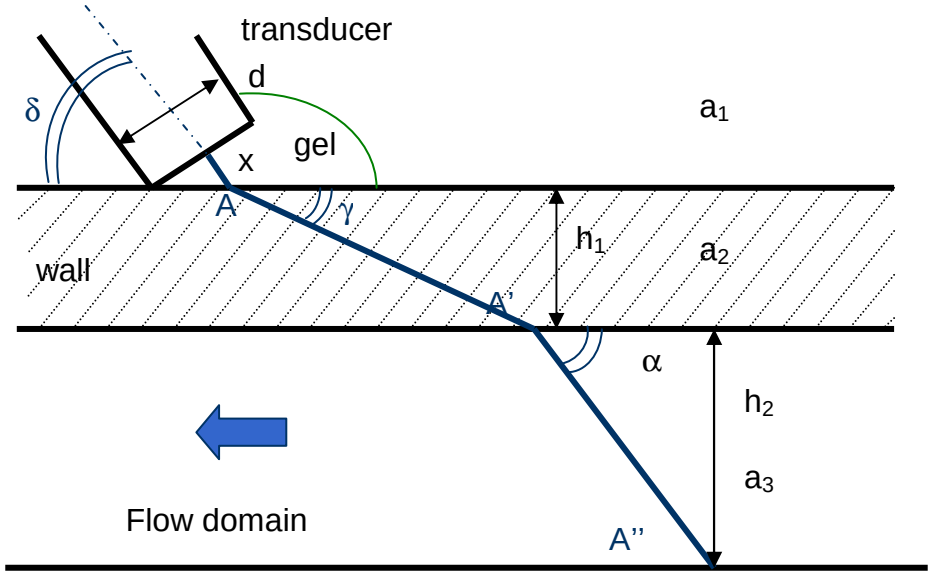

Fig. 3: wall data correction of the echoes' position, function of:

- ***geometrical characteristics of the system (transducer: d; wall: h_1; flow domain: h_2)***
- ***acoustic characteristics of the system (gel's celerity, needed for the coupling transducer-wall: a_1; celerity inside the wall: a_2; celerity inside the flow domain: a_3).***

2) The idea of local velocity measurement referred to a certain distance from the transducer is an ideal concept; in the reality the measurements are mean values of the velocities observed on a finite sampling volume, and the mean value must be referred to the centre of mass of the sample. If we watch the zone close to the wall we have to refer the measurement to the barycentre of the effective sampling volume, therefore to the portion inside the flow (ABCD Fig.4).

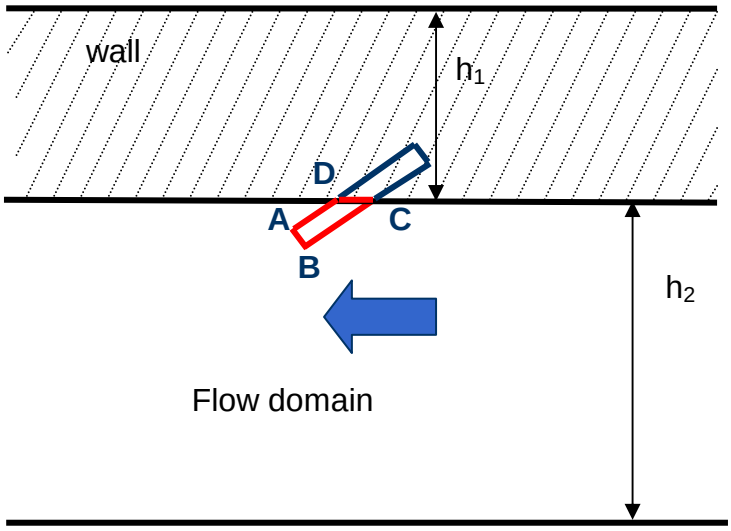

Fig. 4: wall data correction, determination of the effective centre of the sampling volume (Nowak, 2002).

To make this second correction we used the procedure suggested by Nowak (2002) that makes the hypothesis both of plane interface and cylindrical sampling volume with axis equal to "δ", which is admissible considering that the Fresnel's zone is close to the transducer and to the wall.

4. Experimental apparatus

The experiments have been done in a plexiglass channel: length, L = 1m, width, B= 20 cm, height, H= 1cm, available at the "G. Fantoli" Laboratory, Department I.I.A.R. (Politecnico di Milano).
The apparatus has got a fluid feeding system as shown in Fig. 5.

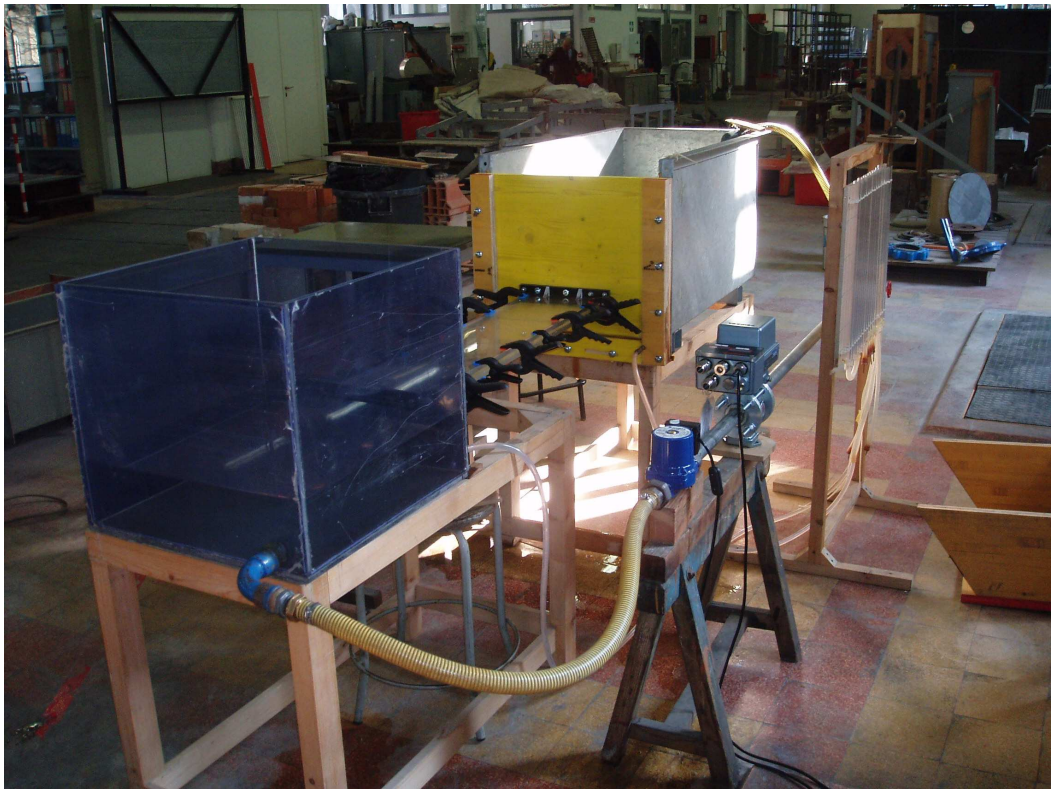

Fig.5: picture of the experimental apparatus.

The velocity profiles have been measured at a section 57 cm far from the inlet characterized by a fully developed flow.
To evaluate the "entrance length" we used as a first approximation the following formula for a turbulent flow:
Entrance length $_{turb}$ = 4,4· $Re^{1/6}$·D
Considering that the cross section is rectangular as D we used 4R with R the hydraulic radius defined as:

$$R = \frac{(BH)}{2(B+H)}$$

At the cross section far from the inlet 70 cm we placed, both on the bottom centre line and on the sidewall centre line, a Preston tube with external diameter (d_{ext}) 1,2 mm, and a ratio between the inner diameter (d_{int}) and the external diameter, equal to 0,67; at the same cross section we placed piezometric intakes of reference.
Building the Preston tube we considered the suggestions Preston the same made (*1954*), and then followed by *Patel* (*1965*); in particular we choose to keep d_{int}/d_{ext} close to the value of 0,6 as the author proposed.
At the cross section far from the inlet 90 cm we placed another piezometric intake that with the ones at 70 cm allows to evaluate the non dimensional pressure drop "J" and therefore the global mean wall shear stress: $\tau_{mean} = \gamma \cdot R \cdot J$.

The measurement of the pressures have been done by a battery of piezometers.
We placed the probe on the external wall of the channel, and we guaranteed the acoustic coupling between the device and the wall using the ultrasonic gel.
The sonic beam has, in this way, to cross two interfaces: gel-wall and wall-flow domain.
About the problems relative the evaluation of the energy reflected and refracted we refer the reader to Nowak (2002); it is clear that the efficiency of the system is conditioned to the type of the materials involved and the angle of incidence, δ. After some preliminary trials we set $\delta = 70°$ as the angle to use during the experiments, result consistent with the remarks done by Nowak 2002.
The device used is *DOP2000* by Signal Processing S.A. (*Signal Processing S.A. DOP 2000 Model 2125 User's manual)*, with a frequency emission of 8 MHz .
During the experiments the time between two subsequent pulses T_{PRF} was in the range 77 -116 μs within a measuring time of about 80s - 2min.
The sampling volume has got a longitudinal resolution of 0,19 mm in water and a constant lateral resolution being the first part of the beam cylindrical ("near field" known as Fresnel's zone) characterized by a length less than 3,3 cm and base circular equal to 5 mm (dimension of the piezoelectric element of the probe).
The near field distance, in fact, is the natural focus of the transducer and a function of the transducer frequency, element diameter (aperture size) and the speed of sound velocity in the medium: for a sound velocity of water of 1,483 m/s at 20 °C and the 8 MHZ transducer it comes that it is characterized by a length less than 33,7 mm.

5. Experimental results

5.1 Experiments on the centre line of the bottom

Fig. 6 shows the axial velocity "u" as a function of the distance from the transducer along the direction of the sound beam.
The Reynolds number has been calculated as:
$Re = V \cdot 4 \cdot R/\nu$ where $V=Q/(B \cdot H)$ being Q the flow discharge measured by a magnetic flow discharge meter placed on the fuel system.
It is possible to recognize a zone inside the flow domain, indicated with the horizontal black arrow, where the sampling volume is completely inside the channel and the measurement is not influenced by the wall effect.
Secondly we can notice that the spurious effect on the velocity measurement (A) induced by the wall placed far from the transducer (TR) is especially evident as is smaller the spatial resolution.

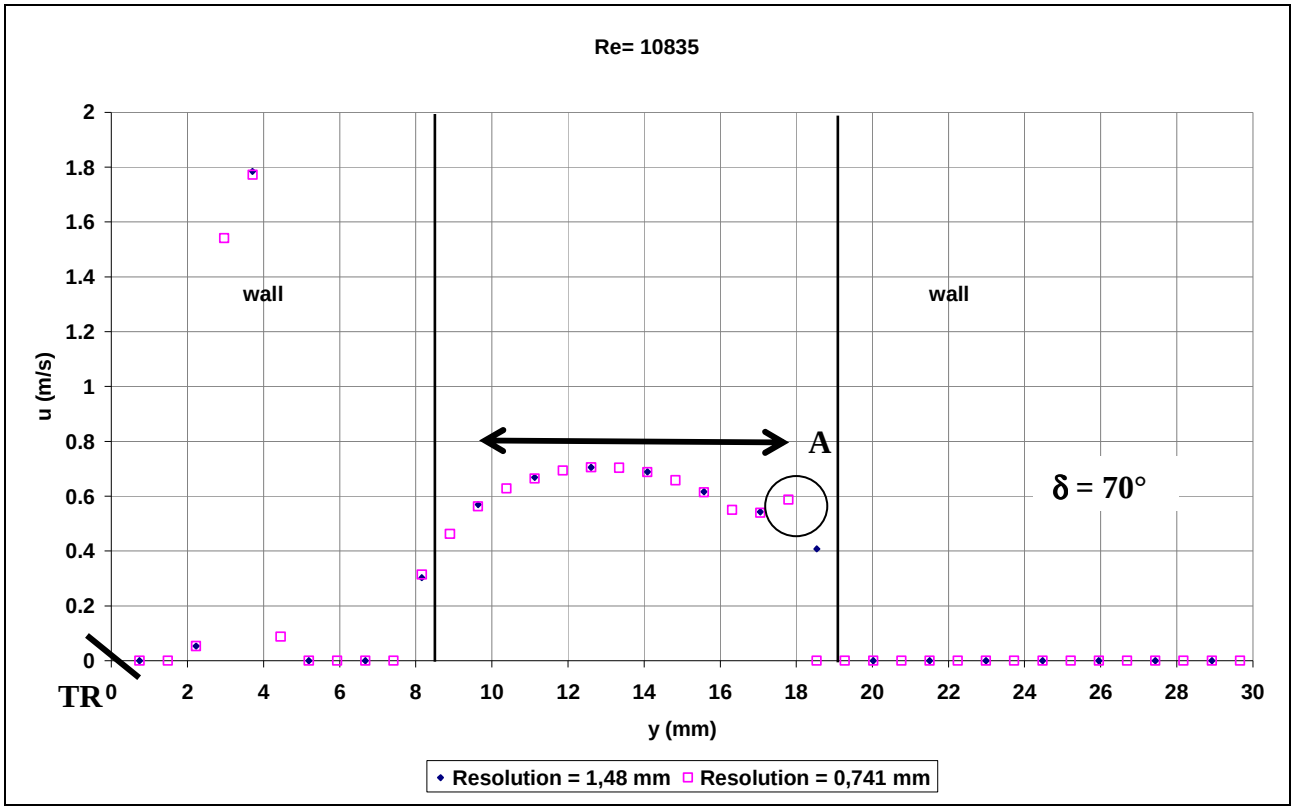

Fig.6 : data referred to the transducer (Re = 10835).

Fig. 7 shows the effect of the Reynolds number on the velocity profile non-dimentionalized respect to the mean velocity. It is interesting to note that there is a different behavior at the increasing of the Reynolds number: for $y < y^*$ at the increasing of the Reynolds number increases the gradient of velocity at the wall while for $y > y^*$ we can see the opposite effect.
This results confirms that even for small Reynolds numbers ($6{,}8 \cdot 10^3 < Re < 10{,}8 \cdot 10^3$) we can see similar behaviors of the flow as those that Zagarola and Smits (1998) found during their experiments ($31 \cdot 10^3 < Re < 35 \cdot 10^6$).

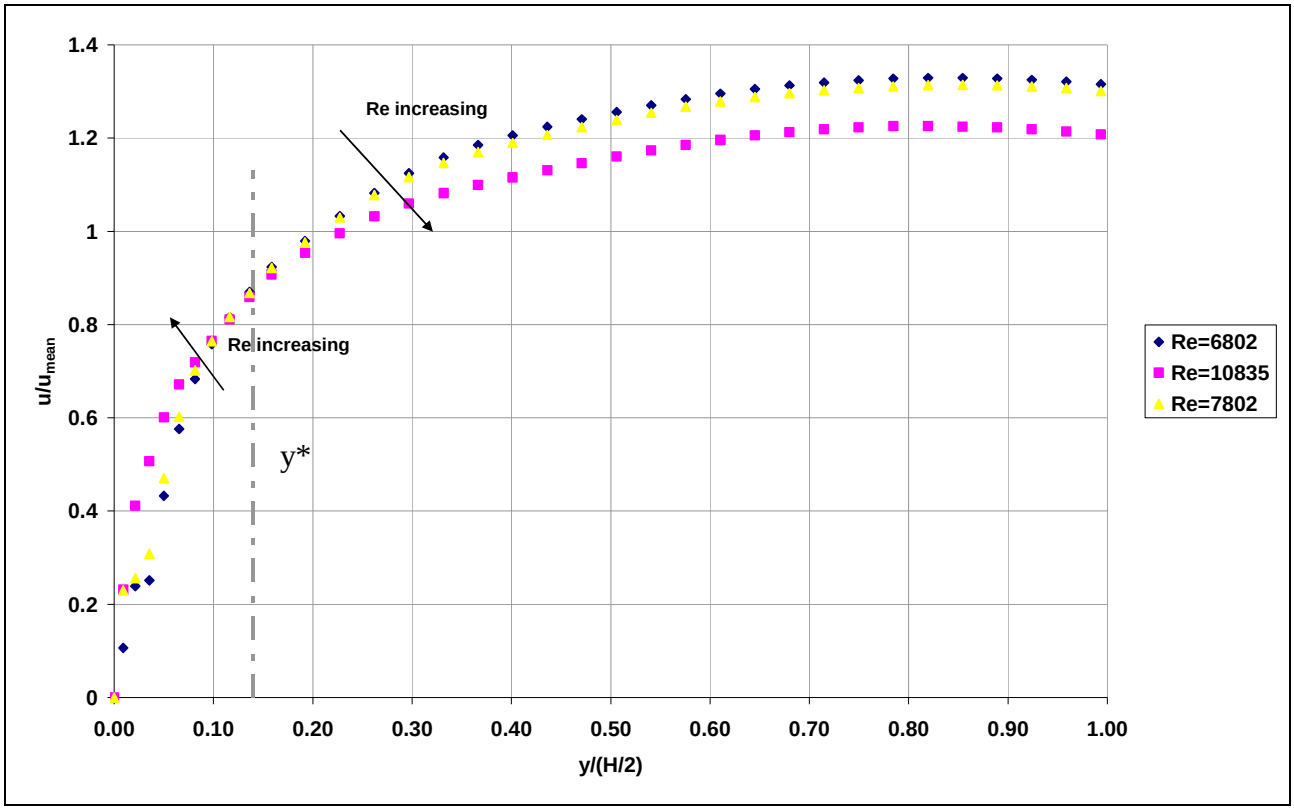

Fig 7: plot showing the velocity profiles normalized by the average velocity for the highest Reynolds number and the lower values of Reynolds number observed during the experiments.

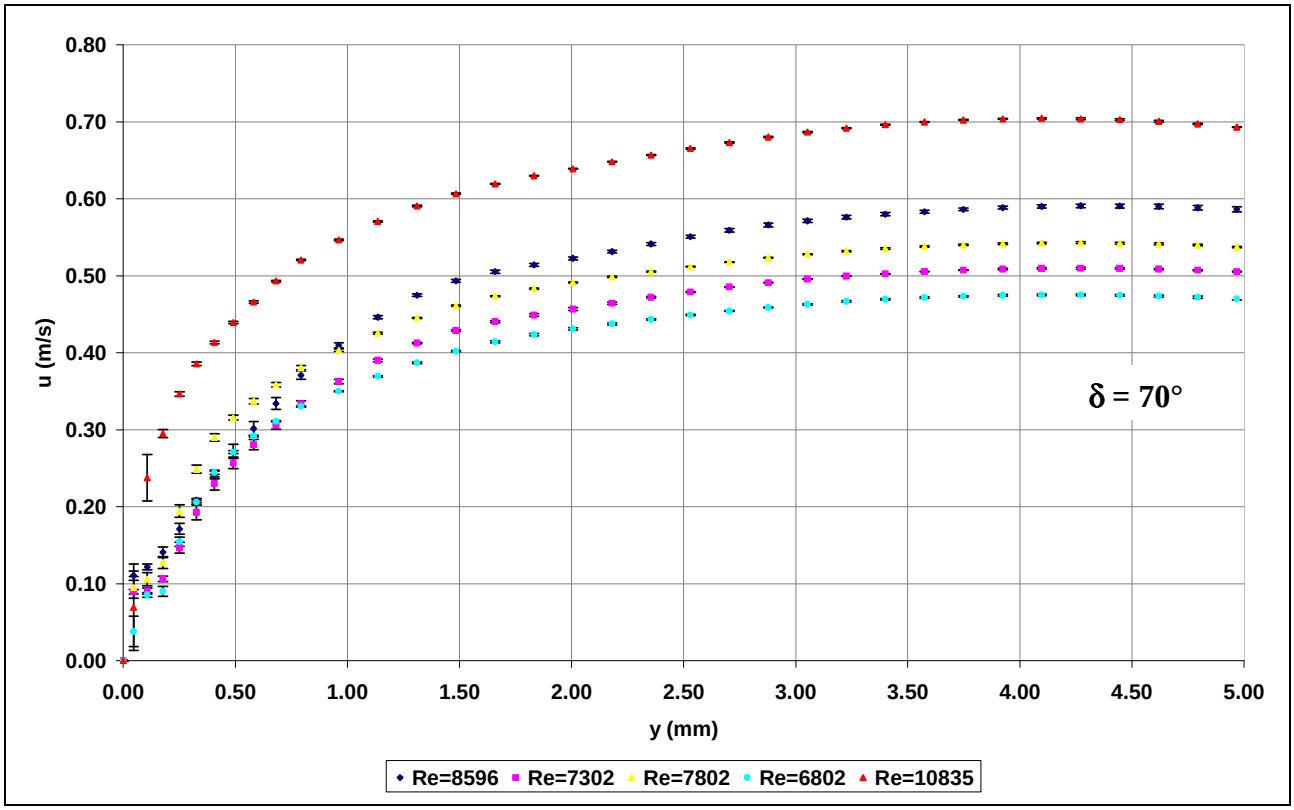

Fig. 8 : water velocity profiles corrected and referred to the wall (y= 5mm defines the axis of symmetry of the channel); every point is obtained by the mean of 4 realization. On the graph has been reported the error bar (±σ – σ = standard deviation) that highlights the critical points located in the wall region.

Fig. 8 shows the mean velocity profiles already referred to the wall; from their analysis we made the normalization with respect to the "inner variables".
Every run has been repeated four times and the total number of the runs is 5, each one is characterized by its own Reynolds number.
The values of the wall shear stresses have been calculated by a linear regression for 3 cases:

- $y^+ \leq 5$ (5 is the well known limiting value for the "viscous sublayer")
- $y^+ < 11{,}6$ (11,6 is the value of interception of the functions described by eq. (1) and eq. (2))
- $y^+ < 8$ (8 is an intermediate value between 5 and 11,6 and it allows to make a regression analysis on at least 3 experimental data points)

Every value of the wall shear stress estimated in this way has been compared to the one estimated by the Preston tube.
The excellent resolution used enabled us to determine the wall shear stress by the analysis of the viscous sublayer while other studies published in literature had to rely on the "log-law" (*Berni et al., 2003*).
This analysis has been done for every value of the Reynolds number both on the single profile and on the mean profile of the four realizations.
It has been confirmed the repeatability of the measurements.
After the results obtained (Tab. 1) we can conclude that the best range of the regression analysis is for $y^+ \leq 5$ because in this case the global mean difference is 14% and it goes down to 9% if we don't take into consideration the run with Re= 10835 (Fig. 9) that is conditioned by a standard deviation of the data points much higher respect to the other runs (Fig. 8).

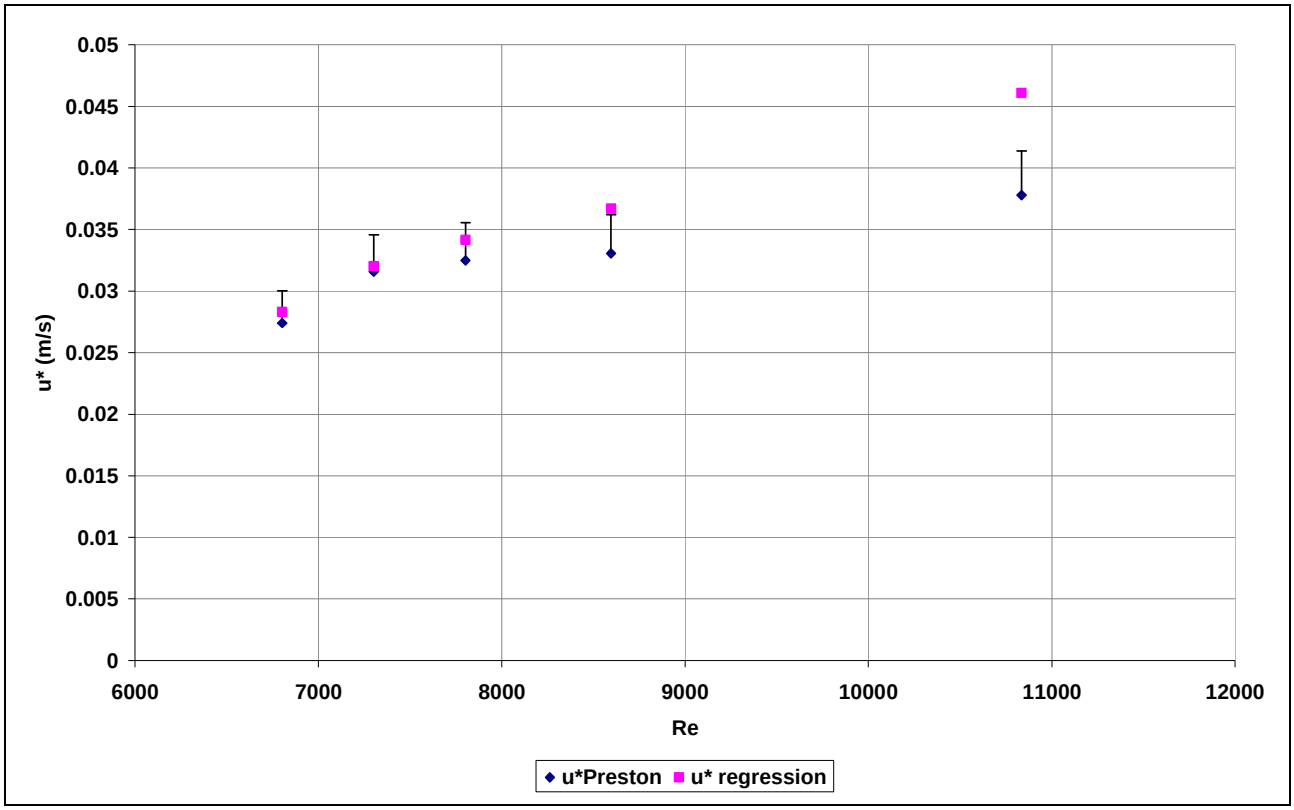

Fig. 9: comparison between u* estimated by a regression and u* measured by a Preston tube; for every data we have reported the 9% error bar.

Re	y^+ limiting value = 11.6	y^+ limiting value = 5	y^+ limiting value = 8
8596	**50,95**	**18,81**	**13,02**
7302	**59,49**	**3,29**	**52,57**
7802	**33,38**	**9,59**	**29,57**
6802	**21,24**	**6,33**	**23,41**
10835	**8,71**	**32,57**	**21,06**
Mean	**34,75**	**14,12**	**27,93**

Tab. 1: differences in % between the absolute value of the wall shear stress measured by a Preston tube and a regression on the velocity profiles varying the limits of integration.

5.2 Experiments on the centre line of the sidewall

In this section we go into depth about the theme of the variation of the wall shear stress on the boundary for a non circular duct.
The measurement of the local wall shear stress (τ_{sw}) have been done by a Preston tube with an external diameter, d_{ext} , of 1,2 mm placed on the center line of the sidewall 70 cm far from the inlet. Patel's calibration curve has been used to calculate the wall shear stress values knowing the pressure difference between the dynamic and the static one done by piezometric readings.
The measurements of the global mean wall shear stress have been derived from the knowledge of the non dimensional pressure drop "J" which has been evaluated by the following formula, where the difference of the piezometric heights is measured by piezometers intakes placed 70 and 90 cm far from the inlet:

$$J = \left(z_{70cm} + \frac{p_{70cm}}{\gamma} \right) - \left(z_{90cm} + \frac{p_{90cm}}{\gamma} \right)$$

$$\tau_{mean} = \gamma \cdot R \cdot J$$

The goals of this analysis have been those that follow:

1) comparison of $\frac{\tau_{CL}}{\tau_{sw}}$, defined the ratio B/H of the cross section, between the case of laminar flow and the case of turbulent flow (here considered);

2) comparison between $\frac{\tau_{local}}{\tau_{mean}}$ here estimated (defined the ratio B/H of the cross section) with that derived from literature data (*Knight et al., 1985*).

5.2.1 Comparison between $\frac{\tau_{CL}}{\tau_{sw}}$ in laminar and turbulent flows

Defined the following scheme in Cartesian coordinates (Fig.10):

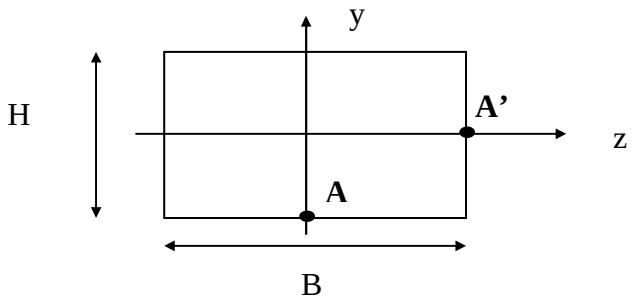

Fig. 10: definition of the scheme of the geometry under study.

It is possible for a laminar flow evaluate the wall shear stress in A (τ_{CL}), and in A' (τ_{sw}) as (*Marchi e Rubatta, 1981*):

$$\tau_{CL} = \frac{\gamma J}{2} H \left\{ 1 - \sum_{k=0}^{\infty} \frac{8}{(2k+1)^2 \pi^2} \cdot \frac{1}{Ch\left[(2k+1)\pi \frac{B}{2H}\right]} \right\}$$

$$\tau_{sw} = \frac{\gamma J}{2} H \sum_{k=0}^{\infty} (-1)^k \frac{8}{(2k+1)^2 \pi^2} Th\left[(2k+1)\pi \frac{B}{2H}\right]$$

From which we can calculate that $\frac{\tau_{CL}}{\tau_{sw}}$ =1,34 for B/H=20 while for the turbulent flow , that is the flow during our experiments, we can observe a certain dependence on the Reynolds number (Re). For the lower values of Re we can approximate the ratio to the one typical for the laminar condition while at the increasing of Re it tends to the unit value (Fig. 11).

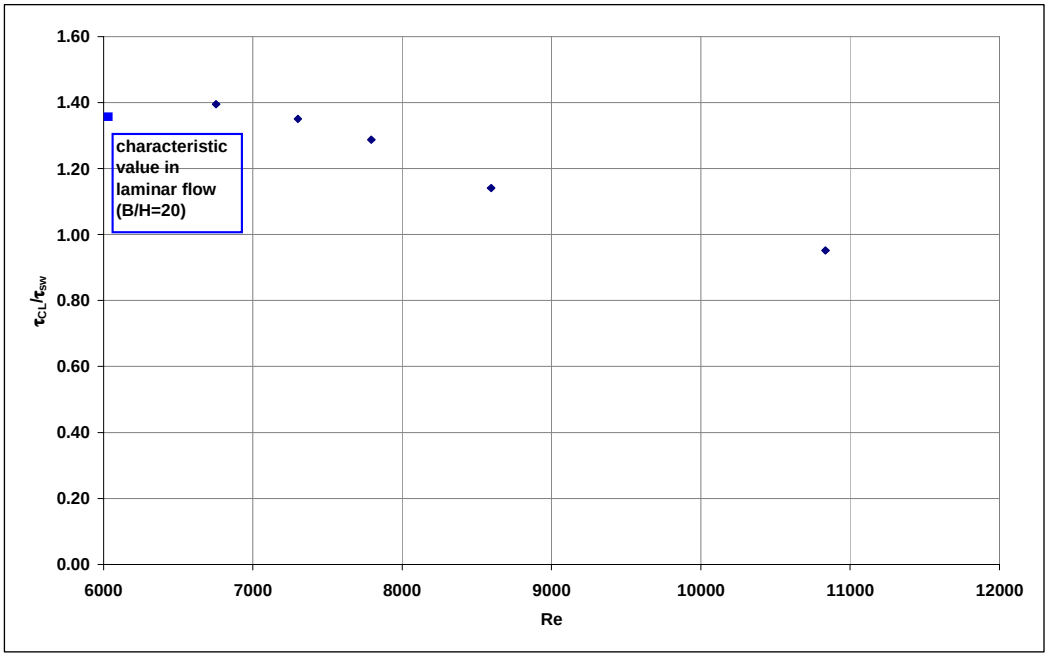

Fig.11: $\frac{\tau_{CL}}{\tau_{sw}}$ ***varying the Reynolds number.***

5.2.2 Comparison between the $\frac{\tau_{local}}{\tau_{mean}}$ on the basis of literature results

To evaluate the effect of the "aspect ratio" we made a comparison between our experimental results and those published in literature.

In particular we made reference to *Knight et al.* (1985), because in the ambit of their study they took into consideration pressure driver flows.

In Fig. 12 we put on a graph *Knight's et al.* experimental results (1985) and ours; the graph shows a good fitting in the mean of our measurements with the previous results.

We considered only the runs: Re=10835 and Re=8596 because our results for lower Reynolds number are too dependent on the error of the estimation of J from which the value of τ_{mean} is calculated.

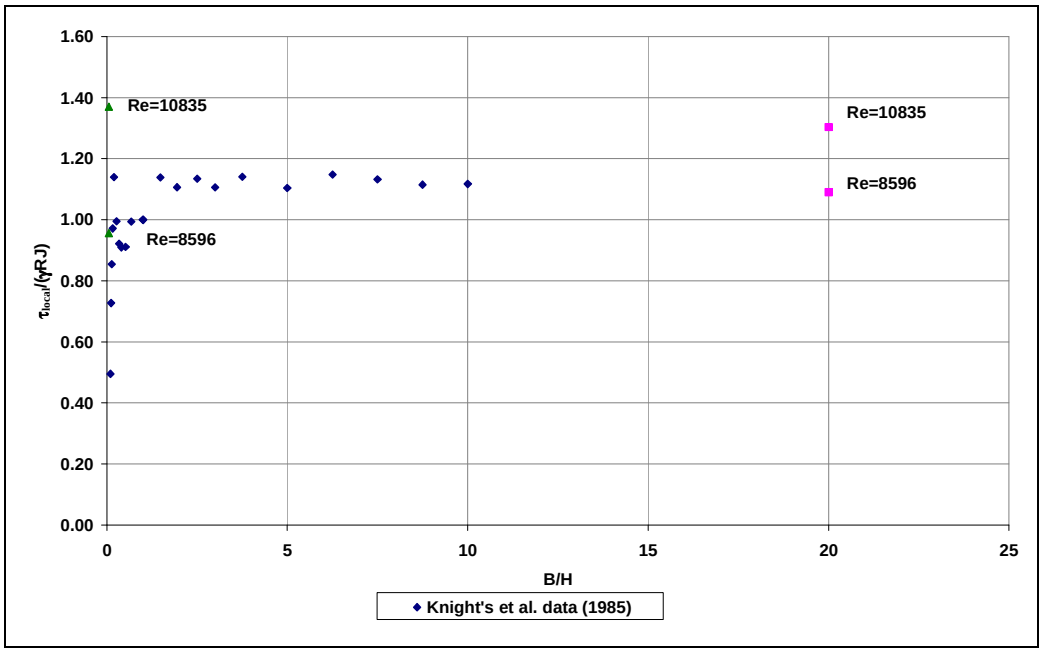

Fig. 12: comparison between our experimental data and the ones published in literature.

6. Conclusions

The possibility to measure velocity profiles with high resolution both in space and in time, and to estimate wall shear stresses by a pulsed UDV has been considered for the Re range: $6{,}8 \cdot 10^3$ - $10{,}8 \cdot 10^3$.
The results confirms that even for small Reynolds numbers ($6{,}8 \cdot 10^3 < Re < 10{,}8 \cdot 10^3$) we can see similar behaviors of the velocity profiles non-dimentionalized as those that Zagarola and Smits (1998) found during their experiments ($31 \cdot 10^3 < Re < 35 \cdot 10^6$).
The friction velocity has been calculated on the basis of a regression analysis of the velocity profile that has been corrected according to the Nowak's procedure within the viscous sublayer.
The mean global error has been of the order of 14% (this value has been strongly conditioned by the run for Re=10835) otherwise it should have been of the order of 9%; in some cases the difference has been of 3% - 6%.
About the variability of the wall shear stress on the boundary, on the basis of the experimental results, we can see that for low values of the Reynolds number (6300) the ratio $\frac{\tau_{CL}}{\tau_{sw}}$ is aligned with the one obtained for a laminar flow and B/H=20 while it decreases at the rising of the turbulence.
The experimental results show a relationship between the ratio of the local wall shear stress and the mean wall shear stress, with the "aspect ratio", as also highlighted by *Knight et al.* (1985).

7. References

1. *Berni, A., Brunone, B., Ferrante, M., (2003), "Rilievi di velocità in una corrente turbolenta mediante tecnica UDV", XI Convegno Nazionale a.i.ve.la., Ancona, 2-3 dicembre.*

2. *Guo, J., Julien, P.Y., (2005), "Shear stress in smooth rectangular open-channel flows", Journal of Hydraulic Engineering, 131(1), 30-37.*

3. *Jin, Y.C., Zarrati, A.R., Zheng, Y., (2004), "Boundary shear distribution in straight ducts and open channels", Journal of Hydraulic Engineering, 130(9), 924-928.*

4. *Kirkgöz, M.S., (1989), "Turbulent velocity profiles for smooth and rough open channel flow", Journal of Hydraulic Engineering, 115(11), 1543-1561.*

5. *Klebanoff, P.S., (1954), "Characteristics of turbulence in a boundary layer with zero pressure gradient" NACA tech note n° 3178, Washington DC.*

6. *Knight, D.W., Demetriou, J.D., Hamed, M.E., (1984), "Boundary shear in smooth rectangular ducts", Journal of Hydraulic Engineering, 110(4), 405-422.*

7. *Knight, D.W., Patel, H.S., (1985), "Boundary shear in smooth rectangular ducts", Journal of Hydraulic Engineering, 111(1), 29-47.*

8. *Marchi, E., Rubatta, A., (1981), "Meccanica dei Fluidi", Ed. UTET – Torino.*

9. *McKeon, B.J. , Li, J., Jiang, W., Morrison, J.F. , Smits, A.J.. (2004), "Further observations on the mean velocity distribution in fully developed pipe flow", Journal of Fluid Mechanics, 501, 135–47.*

10. *Nezu, I., Rodi, W., (1986), "Open channel flow measurements with a laser Doppler anemometer", Journal of Hydraulic Engineering, 112(5), 335-355.*

11. *Nowak, M., (2002), "Wall shear stress measurement in a turbulent pipe flow using ultrasound Doppler velocimetry", Experiments in Fluids, 33, 249–255.*

12. *Österlund, J.M., Johansson, A.V., Nagib, H.M., Hites, M.H., (2000), "A note on the overlap region in turbulent boundary layers", Physics of Fluids, 12, 1–4.*

13. *Patel, V.C., (1965), "Calibration of the Preston tube and limitations on its use in pressure gradients", Journal of Fluid Mechanics, 23, 185-208.*

14. *Preston, J.H., (1954), "The determination of turbulent skin friction by means of Pitot tubes", Journal of Royal Aeronautical Society, 58, 109-121.*

15. *Signal Processing S.A. DOP 2000 Model 2125 User's manual.*

16. *Steffler, P.M., Rajaratnam, N., Peterson, A.W., (1985), "LDA measurements in open channel", Journal of Hydraulic Engineering, 111(1), 119-130.*

17. *Townsend, A.A., (1956), "The structure of turbulent shear flow", Cambridge University Press, New York, N.Y.*

18. *Yang, S.Q., McCorquodale, J.A., (2004), "Determination of boundary shear stress and Reynolds shear stress in smooth rectangular channel flows", Journal of Hydraulic Engineering, 130(5), 458-462.*

19. *Yang, S.Q., (2005), "Interactions of boundary shear stress, secondary currents and velocity", Fluid Dynamics Research, 36 (3), 121-136.*

20. *Zagarola, M.V., Smits, A.J., (1998), " Mean-flow scaling of turbulent pipe flow", Journal of Fluid Mechanics, Vol. 373, 33-79.*

21. *Zanoun, E.S., Durst, F., Nagib, H.M., (2003), "Evaluating the law of the wall in two-dimensional fully developed turbulent channel flows", Physics of Fluids,15, 3079–89.*